NANO LETTERS

Letter

Cite This: Nano Lett. 2019, 19, 7377−7384

pubs.acs.org/NanoLett

Strong Opto-Structural Coupling in Low Dimensional $GeSe_3$ Films

Syed Ghazi Sarwat,[†] Zengguang Cheng, Nathan Youngblood, Mohd Sharizal Alias, Sapna Sinha, Jamie Warner, and Harish Bhaskaran*

Department of Materials, University of Oxford, Oxford OX1 3PH, United Kingdom

Supporting Information

ABSTRACT: Chalcogenide glasses as nanoscale thin films have become leading candidates for several optical and photonic technologies, ranging from reflective displays and filters to photonic memories. Current material systems, however, show strong optical absorption which limits their performance efficiencies and complicates device level integration. Herein, we report sputter deposited thin films of $GeSe_3$, which are low loss and in which the flexible nature of the atomic structure results in thermally activated tunability in the refractive index as well as in the film's physical volume. Such changes, which occur beyond a threshold temperature are observed to be accumulative and directed toward a more equilibrium amorphous state of the film, instead of crystallization. Our results provide insight into a new type of configurability that is based on strong coupling in the material's opto-structural properties. The low optical losses in this material system combined with the tunability in the optical properties in the visible and near-infrared have direct application in higher performing optical coatings and in corrective optics.

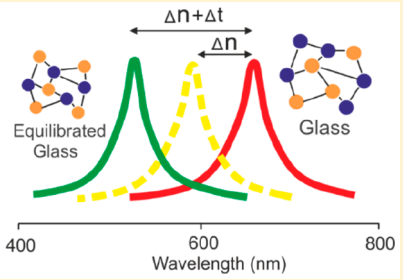

KEYWORDS: *$GeSe_3$, structural relaxation, opto-structural coupling, thin film optics*

Devices which can modulate light on-demand underpin the functionality of several photonic and optical systems, including optical signaling, coatings, and data storage.[1,2] In recent years, one particular class of material, namely the chalcogenide glass (S, Se, Te alloys) has stood-out as a functional material of choice in such technologies.[2,3] In particular, Te-based chalcogenide glasses have enabled all-optical and nonvolatile photonic memories,[4,5] brain-inspired computational architectures,[6,7] artificial retinas,[8] metasurfaces,[9] and more. New device concepts including solid-state displays[10,11] are also closely tied with these remarkable materials. Although promising, these technologies are not yet mature. Minimizing optical losses, which are intrinsic to Te-based chalcogenide glasses[12−14] across a broad wavelength range, is a key goal of research in this field. For example, optical losses in the infrared affect performance efficiencies,[15] such as signal-to-noise ratio in photonic memories, while in the visible it complicates device architectures,[11,16] such as the need for multilayers in reflective displays. Furthermore, optical losses limit the development of several high-performing reconfigurable device concepts, such as interferometers, holograms, spectrometers, and routers. There is, therefore, a growing need for low loss (wide bandgap) materials. Sulfide and selenide chalcogenide glasses are of particular interest due to their ease of manufacture and material science know-how from their commercial use in imaging lenses.[14,17] Selenide glasses are more compelling as a choice due to their properties of reduced toxicity and high chemical and thermal stability.[17,18] The simplest of the selenide glasses are the binary Ge-doped Se (GeSe) compositions. Such compositions currently serve as the parent system for multicomponent alloys, such as the commercially used GLS glasses and phase change materials.[13,14] GeSe glasses show stoichiometric-dependent material properties, such as optical bandgap,[19] amorphization−crystallization reversibility,[20−25] and electronic properties[20,26] and also find application for thermoelectrics,[27,28] data storage,[26] photovoltaics,[29] and catalysis.[29]

Here we report our findings on the optical and structural properties in the nanoscale films of Ge-doped Se glass ($GeSe_3$). Crucially, in our experiments we find low optical absorption in the material and a coupling in its optical and structural properties. We find that past a threshold temperature the material undergoes profound structural changes. Such changes are observed to be accumulative and directed toward a more equilibrium amorphous state. This is different from the Te-based chalcogenide systems, such as phase change materials, where crystallization dominates for similar experimental conditions. Further, notable reductions in the refractive index occur, which we find to be a result of the intrinsic atomic reordering. We collate the structural changes induced optically and thermally in the thin films and compare these effects between nano- and microscale films. We demonstrate that the opto-structural changes in this material could be of interest for applications broadly relating to corrective optics for which these material properties as well as the fabrication means of sputter deposition are well-suited.

Results and Discussion. Thin films of $GeSe_3$ of varying thicknesses were deposited on a variety of substrates: silicon, platinum, gold, quartz, and aluminum foil (see Figure 1) using

Received: July 24, 2019
Revised: August 11, 2019
Published: August 23, 2019

DOI: 10.1021/acs.nanolett.9b03039
Nano Lett. 2019, 19, 7377−7384

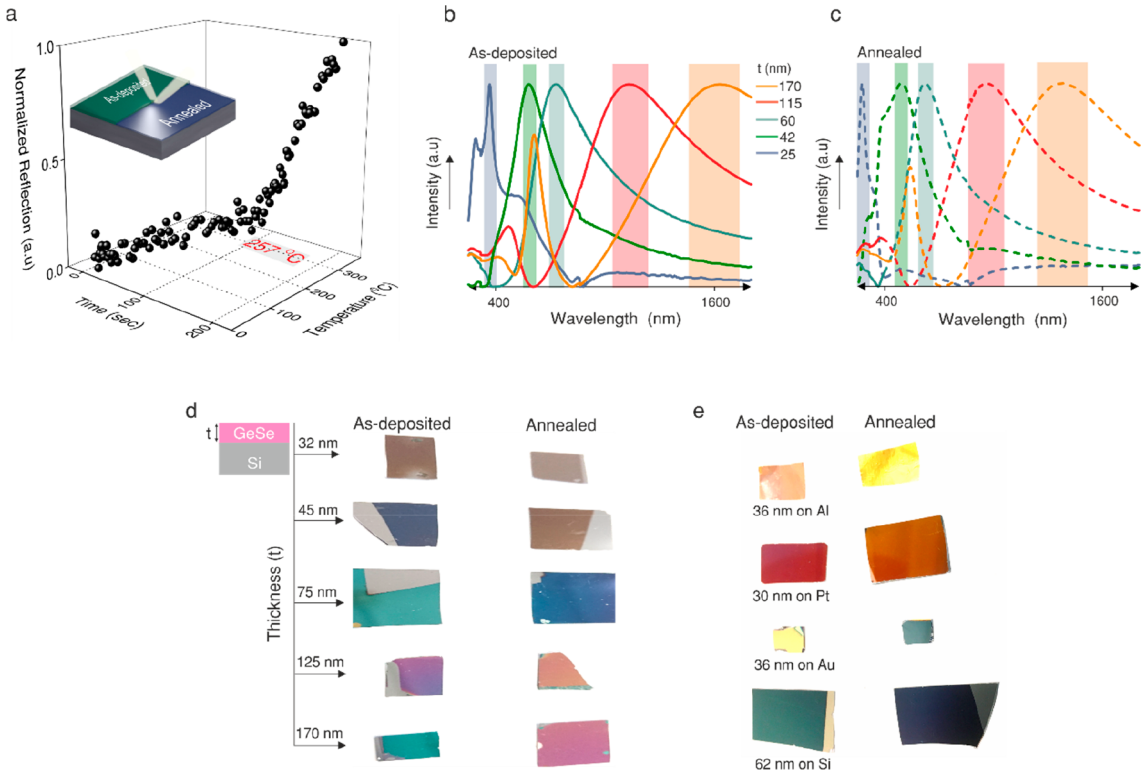

Figure 1. Color changing thin films. (a) Reflection change of a 60 nm $GeSe_3$ thin film on a silicon substrate, as a function of temperature and time. The reflection change translates to a color change of the film, which is illustrated by the sketch in the inset. (b) The reflection spectra of as-deposited $GeSe_3$ thin films of varying thickness on a silicon substrate. The peak position implies optical resonances and varies proportionally with the film thickness. (c) Reflection spectra of the same films after thermal annealing at 370 °C under laboratory conditions for 6 min. The peaks blueshift from thermal treatment. (d) Photographs of five different $GeSe_3$ films of varying thickness on the Si substrate before and after thermal annealing in laboratory conditions. (e) Photographs of $GeSe_3$ thin films on different substrates before and after annealing in laboratory conditions. Note the substrate-dependent coloring and change in color from annealing.

RF-sputter-deposition. The resulting samples display a range of colors, which we find to be dependent on both the thickness of the $GeSe_3$ thin films and the underlying substrate. More importantly, we note that thermal annealing of the as-deposited thin films on a hot plate under ambient conditions brings forth a significant color shift. Similar color changes are observed in reconfigurable Te-based chalcogenide glasses or phase change materials. In phase change materials, this occurs due to the reversible phase transformation of the thin film between its amorphous and crystalline states, which have contrasting optical properties. From the in situ reflectometry measurements (see Figure 1a) of a $GeSe_3$ thin film on a heated stage in laboratory (ambient) conditions, the onset for a change (optical reflection) is observed to occur at 257 °C. The change is gradual and accumulative, unlike in phase change materials, where it is rapid and bistable (see Figure S1). Figure 1b,c illustrates the reflectivity measurements on some of the sputtered films on p-doped Si wafers before and after thermal annealing, respectively. Distinct reflection peaks (optical resonances) that shift to longer wavelengths proportionally with the film's thickness are evident on both figures. However, the resonances significantly blueshift by as much as 27% (see Figure S2 and Figure S3) from annealing. Figure 1d is a photograph of a few $GeSe_3$-coated Si wafers, which, depending on the thickness of the film, exhibit a range of colors. More importantly, thermal annealing (370 °C under laboratory conditions for 6 min) of the samples beyond the onset temperature induces a significant change in the sample colors, visible when incident "white" light is reflected back. The reflected colors of the thin films on different substrates are shown in Figure 1e. Thermal annealing (350 °C under laboratory conditions for 5 min) results in profound changes in the reflected color.

Figure 2a illustrates the refractive indices of a 25 nm $GeSe_3$ thin film in its as-deposited and annealed states (360 °C/6 min/room conditions). The wavelength-dependent refractive index is a complex entity with a real part n (the measure of wave velocity) and an imaginary part k (the measure of optical absorption). In the visible region of the spectra (400−800 nm), n of the film peaks at 2.94 and k at 0.5. The large n enables resonances in ultrathin films, down to thicknesses approaching $\lambda/12$, whereas the small magnitude of the k enables low loss phase accumulation in the film. Both n and k are found to decrease from thermal annealing. Furthermore, we also find a correlative change in the physical volume of the film from annealing. The thickness of the film shrinks by 22% (see Figure 2b) from thermal annealing beyond the onset temperature. On the basis of these observations, the mechanism determining the coloration of the films and the significant peak shifts can be explained simply by approximating the samples as Fabry−Perot type cavities.[30] The resonance condition is then a function of film's thickness and refractive index and approximately follows the relation $\lambda = h \times 4n$ (where h is the thin film thickness). A thermal treatment decreases both the film's thickness and its refractive index. Concomitantly, the summation of these effects means that the

DOI: 10.1021/acs.nanolett.9b03039
Nano Lett. 2019, 19, 7377−7384

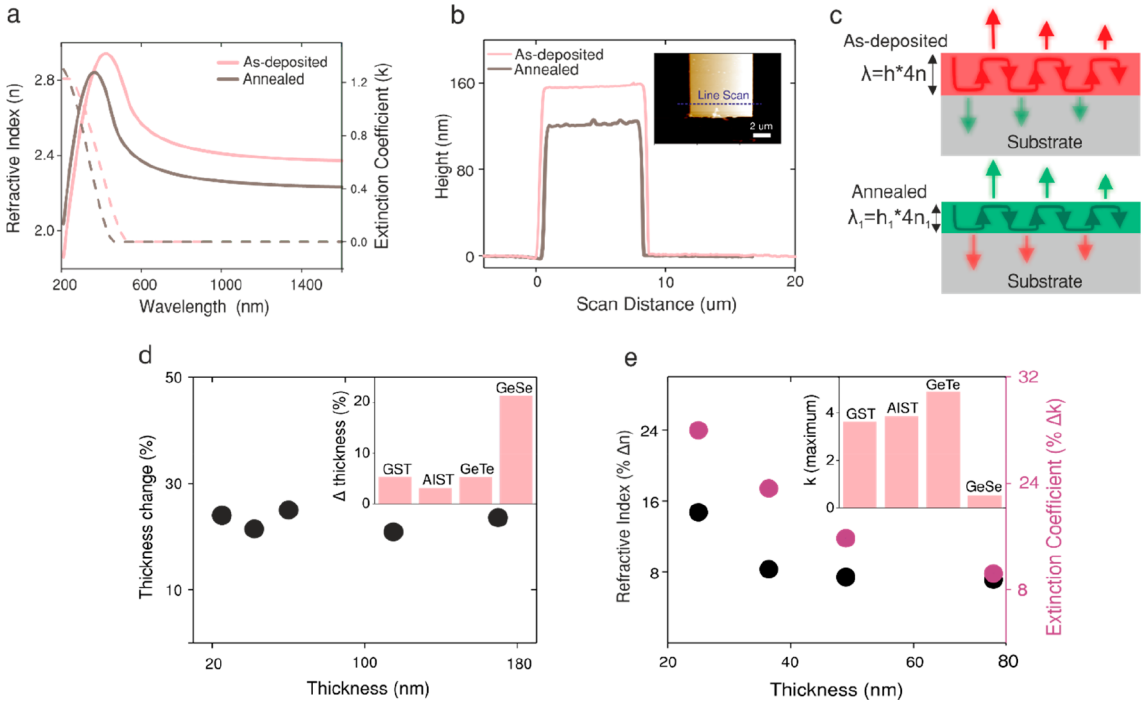

Figure 2. Optical and structural properties. (a) Refractive index of a $GeSe_3$ thin-film in its as-deposited and annealed states. (b) An atomic force microscopy image of a $GeSe_3$ thin-film before and after thermal annealing. The film's thickness reduces by 22%. (c) Schematics illustrating the mechanism of coloration. Optical resonances supported in the film (λ) are a function of both film thickness and refractive index. Annealing results in a nonvolatile decrease in both, which switch the resonances in the film, based on the simple relation $\lambda = h \times 4n$. (d) A scatter plot of the reduction in the thickness of $GeSe_3$ thin-films after annealing as a function of the film thickness. The inset compares the thickness change against other chalcogenide glasses. (e) Variation of the refractive index of $GeSe_3$ thin-films after annealing as a function of the film thickness. These values correspond to wavelengths at which the difference in the extinction coefficient is the greatest. The inset illustrates a comparison of the extinction coefficient (maximum) against other chalcogenide glasses.

resonating wavelengths supported in the films decrease, explaining the blueshifts in the resonance peaks (see Figure 2c) or the reflected color.

We find that the amount of shrinkage is rather independent of the film thickness (see Figure 2d). The inset in Figure 1d compares the percentage of thickness shrinkage in $GeSe_3$ films against commonly used Te-based chalcogenide glasses,[31,32] that is, $Ge_2Sb_2Te_5$, $Ge_{40}Te_{60}$, and AgInSbTe. These materials are deposited and annealed under similar conditions as $GeSe_3$ thin films. Crucially, the $GeSe_3$ thin films show significantly higher volume change. On the contrary, annealing driven changes in the optical properties of the thin films are observed to be thickness dependent (see Figure 2e and Figure S4 for data on other substrates). Compared against other chalcogenide glasses, the k that determines the amount of optical absorption is low in the $GeSe_3$ films (see inset in Figure 2e where peak k value is plotted, which is derived from the ellipsometry measurements shown in Figure S5). To back the mechanism we propose on the coloration of films and the blueshifts, we made samples with lossy $Ge_2Sb_2Te_5$ thin films deposited on Si. Because of the high optical absorption in such films, they colorise only under the conditions of "strong interference", which require reflective substrates,[33] such as metals. We find optical resonances, as well as thermal driven shifts, are absent in the reflection spectra of GST-coated Si samples (see Figure S5a,b). However, we do note that a linear relation as is expected between the degree of peak shift and the material's properties in $GeSe_3$ films does not exist (Figure S3). Such discrepancy could be associated with multiple parameters that are changing at the same time and also with the spurious compounds that form at the interface between the film and the substrate due to interfacial reactions, as are observed in the transmission electron micrographs (TEM) (see Figure S6). Regardless, it is rather interesting to find that the $GeSe_3$ films show changes in their optical properties similar to Te-based chalcogenide glasses.

In order to understand the observed changes in the optical and physical properties, we studied the behavior of the material at the atomic and molecular scale. We find that unlike Te-based chalcogenide glasses, the changes in the optical and structural properties in the $GeSe_3$ thin films are not from simple amorphous to crystalline phase transition.[32] Indeed, for the temperature for which the samples are annealed no crystallization event is observed using X-ray diffraction (see Figure 3a) and Raman spectroscopy studies (see Figure 3). Even TEM measurements, see insets of Figure 3b, show no crystallization. It is therefore hypothesized, in agreement with previous reports on similar macro- and microscale material systems, that the thin films undergo reordering at the atomic scale toward a more stable amorphous phase configuration upon annealing. The fact that the optical properties, which are a function of nearest neighbor stoichiometry, change from annealing indicate that the atomic rearrangements also involve the formation of new bonds. Indeed, this is substantiated on the Raman spectroscopy measurements. Figure 3c highlights Raman spectra of a thin film (90 nm) recorded at low laser power (1.25 mW/532 nm/Spot Size 1 μm) to negate photoannealing (see Figure S7). Signature Raman peaks[34,35] of GeSe alloy are evident and represent various vibrational modes of the alloy (see Figure S8). Structural blocks of GeSe

DOI: 10.1021/acs.nanolett.9b03039
Nano Lett. 2019, 19, 7377−7384

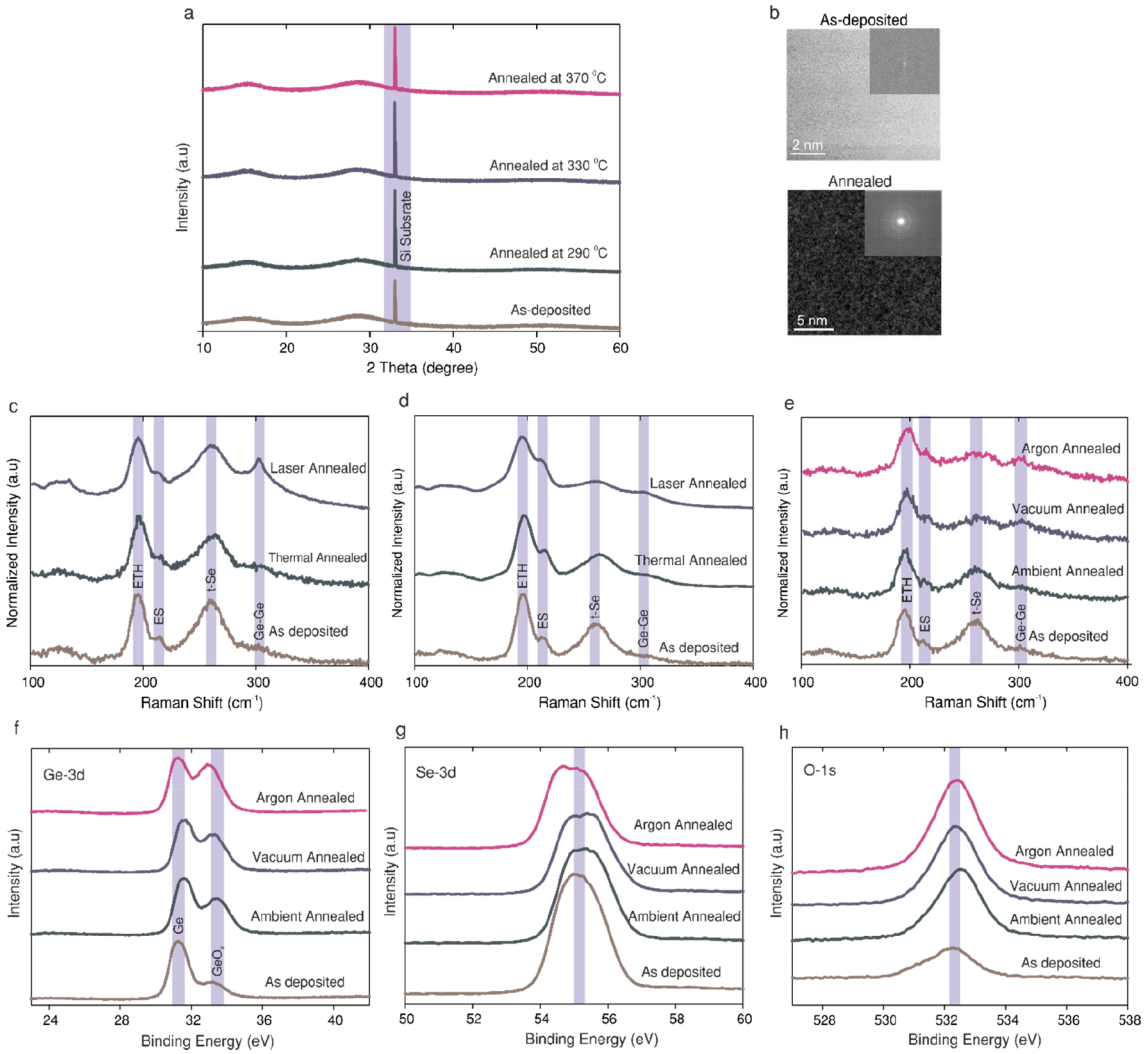

Figure 3. Structural and atomic bond reconfigurations. (a) X-ray diffraction scans of a 1 μm thick $GeSe_3$ film on a silicon substrate in as-deposited and after annealing to different temperatures. No signature peaks indicating crystallization are evident. (b) TEM diffraction patterns of a 160 nm thick film in as-deposited and annealed conditions confirm the amorphous nature of the film in both states. (c) Raman spectra of a 90 nm thick $GeSe_3$ film in as-deposited, thermally annealed (370 °C) and laser annealed conditions. (d) Raman spectra of a 1 μm thick film before and after thermal and optical exposure. (e) Raman spectra of a 75 nm thin film annealed to 370 °C in the room, vacuum, and argon environment. (f) XPS spectra of the prominent Ge 3d and GeO_x peak in the film in the as-deposited and annealed conditions. Annealing results in peak shift in 3d peaks and an increase in the intensity of the GeO_X peak; both indicative of a change in Ge oxidation state. (g) Blueshift in the binding energy is also observed in Se, indicative of spin−orbit splitting and (h) signature O-1s peak. Increase in its intensity is indicative of greater surface oxidation.

alloys are understood to be Ge-centered tetrahedrons and chains and rings of Se. The 194 cm^{-1} corresponds to ETH vibration modes of the corner sharing $GeSe_{4/2}$ tetrahedrons and the companion peak at 211 cm^{-1} represents the ES breathing vibrations of the edge-shared $Ge_2Se_{8/2}$ bitetrahedrons. The peak at 262 cm^{-1} corresponds to the Se−Se bonds and suggests that the predominant configuration of Se is in the form of Se-8 rings. The thermal annealing is observed to induce a decrease in the Se−Se peak intensity. This, however, occurs with an increase in the ES peak intensity (also see Figure S8).

Collectively, these indicate the intrinsic structural changes on annealing includes an increased formation of Ge−Se heteropolar bonds at the expense of homopolar Se−Se bonds.[36] On the contrary, an intense optical exposure (12.5 mW/532 nm/Spot Size 1 μm) is observed to induce segregation effects in such low-dimensional films, instead of structural ordering. Figure 3c illustrates that an intense laser exposure does not favor reconfiguration of Se−Se bonds, instead it gives rise to a new peak at 302 cm^{-1}. This peak corresponds to a vibrational mode of strained Ge−Ge bonds.[37] Similar changes but of smaller magnitudes are also observed in UV-illuminated films (see Figure S9A). Optical exposure to pulsed UV laser (355 nm) is found to ablate the thin films (see Figure S9B). The optical and thermal exposure of thicker films (1 μm), however, causes preferential conversion of the heteropolar bonds to homopolar bonds in line with literature; although there is a discernible hump at 302 cm^{-1}, thicker films are found to be more resilient to segregation effects (see Figure 3d). The contrast in the material's behavior to the optical and thermal response probably arise from beyond thermal effects, such as electronic excitations. The segregation effects are intensified in thinner films, likely due to increased disorder[38] and interfacial stress effects[39] from the substrate.

The effect of the annealing environment on the microstructure of a thin film is illustrated on the Raman spectra in

DOI: 10.1021/acs.nanolett.9b03039
Nano Lett. 2019, 19, 7377−7384

Figure 3e. Similar observations as in Figure 3c stand, however, for samples annealed in a vacuum (10^{-6} Torr) and in an argon atmosphere, the 302 cm^{-1} peak becomes apparent. However, we note that this peak emerges not from thermal annealing, instead from the laser exposure during Raman measurements. The samples annealed in vacuum and argon are found to be more susceptible to photoannealing than the samples annealed in ambient conditions likely due to longer thermal exposure (the thermal time constant of the furnaces are several minutes; in our experiments of vacuum annealing, the samples were heated at 10 °C/min, held at 370 °C for 10 min, and cooled down at 3 °C/min). From X-ray photoelectron spectroscopy measurements, we deduce the chemical changes, which are induced in the films from thermal treatment. The Ge-3d core-level peak (see Figure 3f) of the as-deposited thin film is centered at 31.1 eV, which is in line with the literature. There is an accompanying shoulder peak at 33.2 eV, which is suggestive of GeO_x. Annealing is observed to induce slight peak shifts, but more notably an increase in the GeO_x intensity, which is indicative of surface oxidation.[40] Figure 3g highlights the changes in the Se-3d peak from annealing. There is a blueshift in the peak, which is suggestive of spin−orbit splitting.[40] No signatures of Se−O oxides are observed on the spectra. Along these lines, the intensity of the oxygen-1s peak is observed to increase from annealing (see Figure 3h). The fact that the oxygen concentration in the film increases even when annealing in high vacuum and in argon indicates that the surface of the film is likely enriched with oxygen that diffuses from the bulk of the material during thermal treatment and that oxygen plays a role in the structural changes of the film.

The bandgap of GeSe is known to increase, whereas the refractive index decreases with increased Ge concentration.[41,19] In the amorphous thin films, this essentially translates into more Ge—Se and Ge—O heteropolar bonds[42] at the expense of Ge—Ge and Se—Se bonds. The formation of GeO_x and reordering of the amorphous lattice toward a more entropy driven disordered (equilibrium) disordered state[36,43,44] explain the change in the optical properties of our films[45,46] after annealing (also see Figure S8). Amorphous chalcogenide glasses are characterized by atomic disorder,[47] where disorder implies wrong bonds (mainly homopolar), structural defects, and dangling bonds. Concomitantly, these defects result in several localized states at the edge of the conduction band, which minimizes the optical band gap. Annealing (both thermal and photo) likely provides sufficient activation energy for breakage of wrong bonds (formation of heteropolar bonds), as well as to induce atomic reordering in the short and medium range. These effects result in the annihilation of the localized states, enlarging the optical band gap and decreasing the material volume due to smaller lattice constants of the heteropolar bonds[48,49] (Ge—Se and Ge—O) over homopolar bonds[50] (Ge—Ge and Se—Se chains). The shrinkage in film thickness is also a consequence of the free-volume reduction. Although volume changes in sulfide glasses are well studied, changes in Se glasses are less well-known. There is previous evidence that associates the densification to void annihilation that originates from porous deposition.[51] However, the fact that we observe similar volume contraction in sputtered thin films suggest that the change is intrinsic and likely associated with both bond reordering and mass transport. Indeed, thin films of other chalcogenide glasses of similar thickness deposited under exact conditions do not undergo similar volume change on annealing (see inset in Figure 2d). Furthermore, in multiple TEM cross sections, we find good homogeneity and uniformity in the films under both as-deposited and annealed states (see inset Figure 3b). We also find circular-shaped grains scattered on the annealed films, independent of the annealing environment. We find these grains are both Se rich and are amorphous as the rest of the film using energy dispersive spectroscopy and TEM, respectively (see Figure S10). If crystallization were to occur in the films[25] under our experimental conditions, the material would have undergone phase segregation into crystalline $GeSe_2$ and Se grains.

Having thus established sufficient evidence for the switching characteristics of $GeSe_3$ films we now demonstrate some applications this material could be well-suited for. Figure 4a illustrates the blueshift in the peak position of a 60 nm $GeSe_3$ thin film on a Si substrate from annealing on a hot plate. It is observed that in contrast to Te-based chalcogenide glasses, which are bistable, there exists a considerable dynamic range for tuning the peak position in the $GeSe_3$ films. Essentially, this dictates that the modulation in the reflected color can be achieved simply heating the film to different temperatures (the inset in Figure 4a highlights the 126 nm blueshift in the reflection spectra of the thin film; each shift is nonvolatile). This tunability can be used for artistic effects and temperature sensors, for example, where colors are modulated on thermal treatment.[33] Such a characteristic could also be used in modulating the transmissive properties. The optical transmission through a 72 nm $GeSe_3$ thin film on a quartz substrate before and after annealing is shown in Figure 4b (also see Figure S11). Notably, the film is highly transmissive, and the transmission is observed to increase from thermal treatment. Importantly, with a direct band gap of ∼4.5 eV (see Figure S12) the material is absorpted in the ultraviolet (UV). UV, both type A and B, can be significantly filtered by films as thin as 25 nm (see Figure S13) unlike oxide glasses, such as quartz and borosilicate. Such a coating could simplify the complexity of commercially used antireflection coatings in many biological and electronic devices, including photodetectors, organic solar cells, and lenses.[52−54]

The very low optical absorption in the infrared, yet tunability in the refractive index (real part) of the material, can be exploited in tuning a wide range of photonic devices.[2,5,13,55] For example, propagation modes in waveguides and optical fibers can be modified without losses and in a nonvolatile manner. Figure 4c illustrates an optical racetrack resonator fabricated from etched Si_3N_4 using electron beam lithography (EBL) and reactive ion etching, followed by the deposition of 150 nm $GeSe_3$ film via EBL and RF sputtering. The detailed fabrication process can be found elsewhere.[4−6,55] The optical and structural changes of $GeSe_3$ during annealing affect the effective refractive index (n_{eff}) of the waveguide region with $GeSe_3$ (Si_3N_4/$GeSe_3$) on top, as clearly shown in the inset of Figure 4c. In comparison with a control device without $GeSe_3$ (Figure S14a), the waveguide with $GeSe_3$ as deposited has a higher n_{eff} with the mode center shifted towards $GeSe_3$. This contributes to mode scattering inside the racetrack, affecting the quality factor of the resonator (Q-factor).[56] After annealing, the effective index of Si_3N_4/$GeSe_3$ decreases, which reduces the mode scattering with an increased Q-factor. The transmission spectra after different annealing temperatures are illustrated in Figure 4d. Using Lorentz function to fit each resonant peak,[55] we could obtain the Q-factor of the resonator, shown in Figure 4e and find that the Q-

DOI: 10.1021/acs.nanolett.9b03039
Nano Lett. 2019, 19, 7377−7384

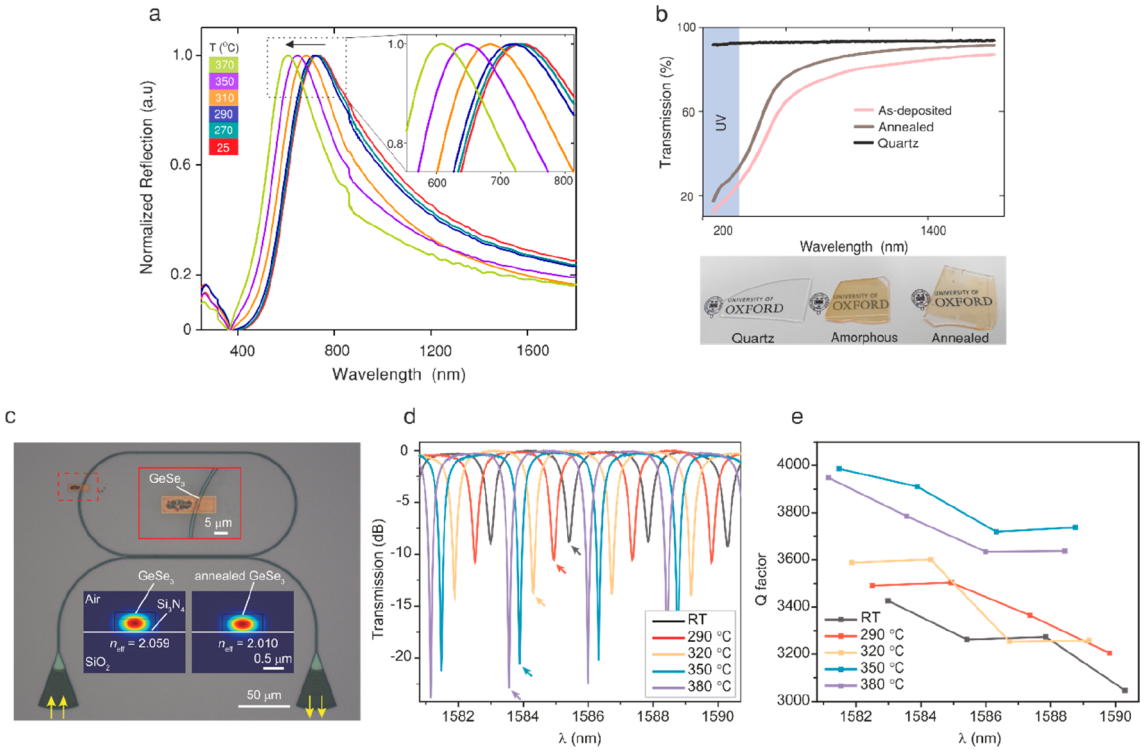

Figure 4. Optical and photonic devices. (a) Accumulative and nonvolatile peaks shifts in a $GeSe_3$ thin film with select annealing temperature. (b) Optical transmission spectra of a 72 nm $GeSe_3$ thin film on a quartz substrate. Annealing at 370 °C in ambient conditions drives a nonvolatile change, making the film more transmissive across all wavelengths. The bottom panel is a photograph of the sample highlighting the increased transmissivity of the sample from thermal treatment. (Permission to use logo granted from Univeristy of Oxford.) (c) Optical micrograph of a photonic race track resonator with a patch of 150 nm $GeSe_3$ thin film (red dashed box). The input and output grating couples of the device are highlighted by the yellow arrows. Bottom inset: Simulations of the mode profile (cross-section) of the waveguide with $GeSe_3$ in the as-deposited and annealed (380 °C) states. n_{eff} is the effective refractive index at the wavelength of 1580 nm. (d) The transmission spectrum of the racetrack resonator shown in (c) at different annealing temperatures. Each curve is normalized to its maximum transmission (RT corresponds to the device before annealing). The arrows show typical resonant peaks of the device with stepwise blueshifts observed as the function of annealing temperature. (e) The calculated Q factor of the device as a function of both the wavelength and annealing temperature.

factor is evidently increased after annealing. On the contrary, the change of the Q-factor of the control device after annealing is not obvious (Figure S14c). Furthermore, the resonance wavelength of the device with $GeSe_3$ could be tuned stepwisely through annealing (Figure 4d). Although the control device shows similar blueshifting of the resonance wavelength after annealing (Figure S14b,d), likely due to the removal of resist residues from fabrication, the magnitude of shifts is small. We obtain the actual wavelength shifts contributed by structural changes in $GeSe_3$ through deducting the shifts in the control devices. We find the effective index change of $Si_3N_4/GeSe_3$ to be 0.0649, slightly higher than the value simulated (0.049) in Figure 4c (see Supporting Information). In addition, the free spectral range (FSR) for both devices are very consistent and not affected by annealing (Figure S15).

Overall, in this article we have explored the material science of nanoscale films of a chalcogenide glass $GeSe_3$. We find that this material system has a wide bandgap, resulting in low optical absorption and that its optical properties are configurable. We show that thermal treatment results in changes in the optical properties of the material, particularly a decrease in the complex refractive index, as well as causes a concurrent reduction in the physical volume. This, as we show, occurs not from a solid to a solid phase change but instead with thermally activated structural changes such as relaxation, which directs the material to a more equilibrated amorphous phase. We apply the low loss characteristic and the coupled opto-structural changes in this material to demonstrate a few applications, broadly relating to corrective optics, which are otherwise less achievable with currently used lossy chalcogenide glasses.

■ ASSOCIATED CONTENT

Supporting Information

The Supporting Information is available free of charge on the ACS Publications website at DOI: 10.1021/acs.nanolett.9b03039.

Reflectivity change in $Ge_2Sb_2Te_5$, Raman spectra of $GeSe_3$, reflection of $Ge_2Sb_2Te_5$ on Si, transmission measurements, compositional analysis, transfer matrix simulations, TEM analysis of interface, exposure to continuous and pulsed UV (PDF)

■ AUTHOR INFORMATION

Corresponding Author

*E-mail: harish.bhaskaran@materials.ox.ac.uk.

ORCID

Jamie Warner: 0000-0002-1271-2019

Harish Bhaskaran: 0000-0003-0774-8110

Present Address

†(S.G.S.) IBM Research, Zurich, Rüschlikon, 8803, Switzerland.

DOI: 10.1021/acs.nanolett.9b03039
Nano Lett. 2019, 19, 7377−7384

Funding

This research was supported by EPSRC via Grants EP/J018694/1, EP/M015173/1, and EP/M015130/1 in the U.K. and from the European Union's Horizon 2020 research and innovation program under Grant Agreement 780848 (FunCOMP project).

Notes

The authors declare the following competing financial interest(s): H.B. holds shares and serves as a company board director at Bodle Technologies Ltd. H.B. is also an employee of the University of Oxford, which may stand to gain both financially and reputationally with published papers.

Additional data may be requested from the Oxford Research Archive for Data (https://ora.ox.ac.uk).

■ ACKNOWLEDGMENTS

S.G.S. acknowledges the Oxford Felix Scholarship that supports his research. This work was primarily supported by EPSRC, European Union's Horizon 2020 programme via the FunComp project and the John Fell Fund. We acknowledge the support of Clement Talagrand, Graham Triggs, Tobias Bachmann and Simon Henley for assistance in experiments.

■ REFERENCES

(1) Smit, M.; van der Tol, J.; Hill, M. Moore's Law in Photonics. *Laser Photon. Rev.* **2012**, *6*, 1−13.

(2) Wuttig, M.; Bhaskaran, H.; Taubner, T. Phase-Change Materials for Non-Volatile Photonic Applications. *Nat. Photonics* **2017**, *11*, 465−476.

(3) Sarwat, S. G.; Youngblood, N.; Au, Y.-Y.; Mol, J. A.; Wright, C. D.; Bhaskaran, H. Engineering Interface-Dependent Photoconductivity in Ge2Sb2Te5 Nanoscale Devices. *ACS Appl. Mater. Interfaces* **2018**, *10*, 44906−44914.

(4) Ríos, C.; Stegmaier, M.; Hosseini, P.; Wang, D.; Scherer, T.; Wright, C. D.; Bhaskaran, H.; Pernice, W. H. P. Integrated All-Photonic Non-Volatile Multi-Level Memory. *Nat. Photonics* **2015**, *9*, 725−732.

(5) Cheng, Z.; Ríos, C.; Youngblood, N.; Wright, C. D.; Pernice, W. H. P.; Bhaskaran, H. Device-Level Photonic Memories and Logic Applications Using Phase-Change Materials. *Adv. Mater.* **2018**, *30*, 1802435.

(6) Cheng, Z.; Rios, C.; Pernice, W. H. P.; Wright, C. D.; Bhaskaran, H. On-Chip Photonic Synapse. *Sci. Adv.* **2017**, *3*, e1700160.

(7) Chakraborty, I.; Saha, G.; Sengupta, A.; Roy, K. All-Photonic Phase Change Spiking Neuron: Toward Fast Neural Computing Using Light. *Sci. Rep.* **2018**, *8*, 1−9.

(8) Sarwat, S. G.; Hernandez, G. R.; Bhaskaran, H. Optoelectronic Device Using a Phase Change Material. PCT/GB2018/051198, 2018.

(9) Raeis-Hosseini, N.; Rho, J. Metasurfaces Based on Phase-Change Material as a Reconfigurable Platform for Multifunctional Devices. *Materials* **2017**, *10*, 1046.

(10) Hosseini, P.; Wright, C. D.; Bhaskaran, H. An Optoelectronic Framework Enabled by Low-Dimensional Phase-Change Films. *Nature* **2014**, *511*, 206−211.

(11) Broughton, B.; Bandhu, L.; Talagrand, C.; Garcia-Castillo, S.; Yang, M.; Bhaskaran, H.; Hosseini, P. Solid-State Reflective Displays (SRD ®) Utilizing Ultrathin Phase-Change Materials. *Dig. Tech. Pap. - Soc. Inf. Disp. Int. Symp.* **2017**, *48*, 546−549.

(12) Dong, W.; Liu, H.; Behera, J. K.; Lu, L.; Ng, R. J. H.; Sreekanth, K. V.; Zhou, X.; Yang, J. K. W.; Simpson, R. E. Wide Bandgap Phase Change Material Tuned Visible Photonics. *Adv. Funct. Mater.* **2019**, *29*, 1806181.

(13) Zhang, Y.; Chou, J. B.; Li, J.; Li, H.; Du, Q.; Zhou, S.; Shalaginov, M. Y.; Fang, Z.; Zhong, H.; Robinson, P.; et al. Extreme Broadband Transparent Optical Phase Change Materials for High-Performance Nonvolatile Photonics. *arXiv Prepr* **2018**, *7014*, 1−16.

(14) Ravagli, A.; Craig, C.; Alzaidy, G. A.; Bastock, P.; Hewak, D. W. Optical, Thermal, and Mechanical Characterization of Ga2Se3-Added GLS Glass. *Adv. Mater.* **2017**, *29*, 1606329.

(15) Li, X.; Youngblood, N.; Ríos, C.; Cheng, Z.; Wright, C. D.; Pernice, W. H. P.; Bhaskaran, H. Fast and Reliable Storage Using a 5 Bit, Nonvolatile Photonic Memory Cell. *Optica* **2019**, *6*, 1−6.

(16) Yu, Y. A. L.; Ou, S. H. M.; Higang, Z. N. I.; Ai, Y. U. B.; Ing, Y.; Un, S.; Heng, Z. H. C. Multi-Color Modulation of Solid-State Display Based on Thermally Induced Color Changes of Indium Tin Oxide and Phase Changing Materials. *Opt. Express* **2017**, *25*, 1405−1412.

(17) Calvez, L. Chalcogenide Glasses and Glass-Ceramics: Transparent Materials in the Infrared for Dual Applications. *C. R. Phys.* **2017**, *18*, 314−322.

(18) Alexander, V.; Kolobov, J. T. Chalcogenides: Metastability and Phase Change Phenomena; **2012**.

(19) Yang, G.; Gueguen, Y.; Sangleboeuf, J.-C.; Rouxel, T.; Boussard-Plédel, C.; Troles, J.; Lucas, P.; Bureau, B. Physical Properties of the GexSe1-x Glasses in the $0 < x < 0.42$ Range in Correlation with Their Structure. *J. Non-Cryst. Solids* **2013**, *377*, 54−59.

(20) Bosse, J. L.; Grishin, I.; Gyu Choi, Y.; Cheong, B.; Lee, S.; Kolosov, O. V.; Huey, B. D. Nanosecond Switching in GeSe Phase Change Memory Films by Atomic Force Microscopy. *Appl. Phys. Lett.* **2014**, *104*, 053109.

(21) Soref, R.; Hendrickson, J.; Liang, H.; Majumdar, A.; Mu, J.; Li, X.; Huang, W.-P. Electro-Optical Switching at 1550 Nm Using a Two-State GeSe Phase-Change Layer. *Opt. Express* **2015**, *23*, 1536−1546.

(22) Griffiths, J. E.; Espinosa, G. P.; Remeika, J. P.; Phillips, J. C. Reversible Reconstruction and Crystallization of GeSe2 Glass. *Solid State Commun.* **1981**, *40*, 1077−1080.

(23) Campbell, K. A. Forced Ion Migration for Chalcogenide Phase Change Memory Device. **2011**.

(24) Letter, P. R. Physical Review Letter. **1986**, *57*.

(25) Cros, B.; Dubourg, M.; Martinez, J. P.; Balladore, J. L. Transmission Electron Microscopy Study of Crystallization on Plasma-Deposited Ge-Se Films. *Thin Solid Films* **1991**, *205*, 13−19.

(26) Shin, S.-Y.; Choi, J. M.; Seo, J.; Ahn, H.-W.; Choi, Y. G.; Cheong, B.; Lee, S. The Effect of Doping Sb on the Electronic Structure and the Device Characteristics of Ovonic Threshold Switches Based on Ge-Se. *Sci. Rep.* **2015**, *4*, 7099.

(27) Ding, G.; Gao, G.; Yao, K. High-Efficient Thermoelectric Materials: The Case of Orthorhombic IV-VI Compounds. *Sci. Rep.* **2015**, *5*, 9567.

(28) Roychowdhury, S.; Samanta, M.; Perumal, S.; Biswas, K. Germanium Chalcogenide Thermoelectrics: Electronic Structure Modulation and Low Lattice Thermal Conductivity. *Chem. Mater.* **2018**, *30*, 5799−5813.

(29) Xue, D.-J.; Liu, S.-C.; Dai, C.-M.; Chen, S.; He, C.; Zhao, L.; Hu, J.-S.; Wan, L.-J. GeSe Thin-Film Solar Cells Fabricated by Self-Regulated Rapid Thermal Sublimation. *J. Am. Chem. Soc.* **2017**, *139*, 958−965.

(30) Ji, H.-K.; Tong, H.; Qian, H.; Hui, Y.-J.; Liu, N.; Yan, P.; Miao, X.-S. Non-Binary Colour Modulation for Display Device Based on Phase Change Materials. *Sci. Rep.* **2016**, *6*, 39206.

(31) Zhou, X.; Dong, W.; Zhang, H.; Simpson, R. E. A Zero Density Change Phase Change Memory Material: GeTe-O Structural Characteristics upon Crystallisation. *Sci. Rep.* **2015**, *5*, 11150.

(32) Sarwat, S. G. Materials Science and Engineering of Phase Change Random Access Memory. *Mater. Sci. Technol.* **2017**, *33*, 1890.

(33) Kats, M. A.; Blanchard, R.; Genevet, P.; Capasso, F. Nanometre Optical Coatings Based on Strong Interference Effects in Highly Absorbing Media. *Nat. Mater.* **2013**, *12*, 20−24.

(34) Olivier, M.; Tchahame, J. C.; Nemec, P.; Chauvet, M.; Besse, V.; Cassagne, C.; Boudebs, G.; Renversez, G.; Boidin, R.; Baudet, E. Structure, Nonlinear Properties, and Photosensitivity of (GeSe 2) 100-x (Sb 2 Se 3) x Glasses. *Opt. Mater. Express* **2014**, *4*, 525.

(35) Porezag, D. V.; Pederson, M. R. Raman-Active Modes of a-GeSe2 and a-GeS2: A First-Principles Study. *Phys. Rev. A: At., Mol., Opt. Phys.* **1999**, *60*, 2840.

DOI: 10.1021/acs.nanolett.9b03039
Nano Lett. 2019, 19, 7377−7384

(36) Yan, Q.; Jain, H.; Ren, J.; Zhao, D.; Chen, G. Effect of Photo-Oxidation on Photobleaching of GeSe2 and Ge2Se3 Films. *J. Phys. Chem. C* **2011**, *115*, 21390−21395.
(37) Lee, M.; Chen, P. The Investigation of Selective Pre-Pattern Free Self-Assembled Ge Nano-Dot Formed by Excimer Laser Annealing. *Nanoscale Res. Lett.* **2012**, *7*, 1.
(38) Kumar, R. T. A.; Qamhieh, N. N.; Mahmoud, S. T.; Lekha, P. C.; Jeyadheepan, K.; Sanjeeviraja, C.; Padiyan, D. P. Evolution of Structural Disorder in Amorphous GeSeS Thin Films by Thickness Variation. *J. Non-Cryst. Solids* **2016**, *450*, 135−140.
(39) Cammarata, R. C. Surface and Interface Effects in Thin Films. *Prog. Surf. Sci.* **1994**, *46*, 1−38.
(40) Mukherjee, B.; Murali, G.; Lim, S. X.; Zheng, M.; Tok, E. S.; Sow, C. H. Direct Laser Micropatterning of GeSe2 Nanostructures Film with Controlled Optoelectrical Properties. *RSC Adv.* **2014**, *4*, 10013−10021.
(41) Wei, W.-H.; Fang, L.; Shen, X.; Wang, R.-P. Transition Threshold in GexSb10Se90-x Glasses. *J. Appl. Phys.* **2014**, *115*, 113510.
(42) Kumar, R. T. A.; Lekha, P. C.; Sundarakannan, B.; Padiyan, D. P. Influence of Thickness on the Optical Properties of Amorphous GeSe2 Thin Films: Analysis Using Raman Spectra, Urbach Energy and Tauc Parameter. *Philos. Mag.* **2012**, *92*, 1422−1434.
(43) Afify, N. Structural Relaxation of ${\mathrm{GeSe}}_{2}$ Chalcogenide Glass Studied with Use of the Radial Distribution Function. *Phys. Rev. B: Condens. Matter Mater. Phys.* **1993**, *48*, 16304−16309.
(44) Lucas, P.; Doraiswamy, A.; King, E. A. Photoinduced Structural Relaxation in Chalcogenide Glasses. *J. Non-Cryst. Solids* **2003**, *332*, 35−42.
(45) Zhang, S.; Chen, Y.; Wang, R.; Shen, X.; Dai, S. Observation of Photobleaching in Ge-Deficient Ge16.8Se83.2 Chalcogenide Thin Film with Prolonged Irradiation. *Sci. Rep.* **2017**, *7*, 14585.
(46) Wang, Y.; Matsuda, O.; Inoue, K.; Murase, K. Photo-Induced Crystallization in Amorphous GeSe2studied by Raman Scattering. *J. Non-Cryst. Solids* **1998**, *227−230*, 728−731.
(47) Kolobov, A. V.; Tominaga, J. *Chalcogenides: Metastability and Phase Change Phenomena*; Springer, 2012; Vol. *164*.
(48) Sahnoun, M.; Daul, C.; Khenata, R.; Baltache, H. Optical Properties of Germanium Dioxide in the Rutile Structure. *Eur. Phys. J. B* **2005**, *45*, 455−458.
(49) Li, Z.-Y.; Liu, M.-Y.; Huang, Y.; Chen, Q.-Y.; Cao, C.; He, Y. Tuning the Electronic Properties of Bilayer Group-IV Monochalcogenides by Stacking Order, Strain and an Electric Field: A Computational Study. *Phys. Chem. Chem. Phys.* **2018**, *20*, 214−220.
(50) Virginia Semiconductor. *General Properties of Si, Ge, SiGe, SiO_2 and Si_3N_4*. **2006**.
(51) Pan, R. K.; Tao, H. Z.; Zang, H. C.; Zhao, X. J.; Zhang, T. J. Annealing Effects on the Structure and Optical Properties of $GeSe_2$ and $GeSe_4$ Films Prepared by PLD. *J. Alloys Compd.* **2009**, *484*, 645−648.
(52) Cook, P. L.; Johnson, P. S.; Liu, X.; Chin, A.; Himpsel, F. J.; Cook, P. L.; Johnson, P. S.; Liu, X.; Chin, A.; Himpsel, F. J. Radiation Damage in Biomimetic Dye Molecules for Solar Cells Radiation Damage in Biomimetic Dye Molecules for Solar Cells. *J. Chem. Phys.* **2009**, *131*, 214702.
(53) Lindström, G. Radiation Damage in Silicon Detectors. *Nucl. Instrum. Methods Phys. Res., Sect. A* **2003**, *512*, 30−43.
(54) Andrady, A. L.; Hamid, S. H.; Hu, X.; Torikai, A. Effects of Increased Solar Ultraviolet Radiation on Materials. *J. Photochem. Photobiol., B* **1998**, *46*, 96−103.
(55) Rios, C.; Hosseini, P.; Wright, C. D.; Bhaskaran, H.; Pernice, W. H. P. On-Chip Photonic Memory Elements Employing Phase-Change Materials. *Adv. Mater.* **2014**, *26*, 1372−1377.
(56) Bogaerts, W.; De Heyn, P.; Van Vaerenbergh, T.; De Vos, K.; Kumar Selvaraja, S.; Claes, T.; Dumon, P.; Bienstman, P.; Van Thourhout, D.; Baets, R. Silicon microring resonators. *Laser Photonics Rev.* **2012**, *6*, 47−73.

DOI: 10.1021/acs.nanolett.9b03039
Nano Lett. 2019, 19, 7377−7384